Differential Behavior of Vectors infected with Chagas' Disease

MTBI-02-12M

Karyn Sutton[1], Priscilla Greenwood[1],

Christopher Kribs-Zaleta[2], Leon Arriola[3]

Carlos Castillo-Chavez[1]

[1] Department of Mathematics and Statistics, Arizona State University, Tempe, AZ

[2] Department of Mathematics, University of Texas at Arlington, Arlington, TX

[3] Department of Mathematical and Computer Sciences,University of Wisconsin at Whitewater, Whitewater, WI

Abstract

Chagas' disease, caused by certain strains of the parasite *Trypanosoma cruzi*, is a vector-borne disease, previously thought to be transmitted solely through the fecal matter of the triatomine vectors after feeding on the mammalian host. However, this mode of transmission is inefficient in the vectors, *Triatoma Sanguisuga* a subspecies of the reduviid family, prevalent in the Southeastern United States, due to the significant delay between feeding and defecation times. The prevalence in this region, 40-60% thus necessitates an alternative explanation. The hosts in the sylvatic cycle of this region, including opossums, raccoons, and armadillos, to name a few, are known to consume the vectors, although this is a traditionally inefficient way of transmitting the parasite. Recently, vector behavior has been observed to be modified during infection, termed differential behavior, such as feeding more frequently and wandering into broad daylight. The extent to which this affects the disease dynamics warrants investigation and could explain the persistence of *T. Cruzi* in the sylvatic cycle of this region. To include both modes of transmission, a deterministic model of the disease dynamics has been developed, incorporating both vector-host and predator-prey dynamics. This model is studied to examine how the differential behavior affects the disease dynamics, threshold of infection, and the current endemic equilibrium which is presently the case. Numerical simulations are carried out to verify the theoretical results. We have shown that elevation of consumption of the vector decreases infection levels and could possibly drive the vector population to extinction. Vectors increased vulnerability to predation increases consumption of infected vectors, which decreases prevalence levels but only slightly affects the total population size. Also, increased feeding frequency of the vectors boosts infection levels significantly, and could explain the high prevalence of *T. Cruzi* in the southeastern United States.

1 Introduction

Chagas' disease is a widely underdiagnosed parasitic infection caused by some strains of *Trypanosoma Cruzi*, or *T. Cruzi*, known to afflict about 16 to 18 million people per year with an estimated 100,000 of these in the United States [5], [6]. Of these, about 50,000 die of the disease [5], typically of cardiac or respiratory complications after chronic infection. This well-established parasite, perhaps predating the arrival of humans [1], [2], is largely prevalent in Latin America and other sufficiently warm climates, and has evolved to establish multiple transmission modes.

The vector-borne disease is transmitted through many species of mammals, including opossums, raccoons, and armadillos as well as humans. Having so many carriers aids the parasite in maintaining high prevalence levels (about 30-60 % in Latin America [3]). In addition to being prevalent in Latin America, some species of the parasites' vector, the reduviid bug which is a member of the Triatominae family, are prevalent throughout the southeastern and in parts of the southwestern United States. This vector is typically found in dark, cool places and feeds on their mammalian hosts, usually during sleep, and passes the parasite through defecation, shed on the host soon after finishing a meal. A host then typically scratches the irritated area, rubbing the fecal matter into its bloodstream by way of broken skin. As a consequence of the vector characteristics, infection is spread to humans via this transmission cycle typically in areas of urban sprawl and/or where there are many buildings and housing establishments of poor construction.

The parasites typically thrive in a sylvatic vector-host transmission cycle - meaning that they are transmitted from the vectors to an animal indigenous to a wooded area and vice versa. This system is largely unstudied, although it has the potential to shed substantial light on this incredibly tenacious parasite. The sylvatic cycle has proven to be a major player in the story of Chagas' disease, with observed prevalence levels of about 40 - 60% [8] in the southeastern United States. This is puzzling, however, since the vectors prevalent in this region have a large delay between feeding and defecation times [9], [10], and merits investigation. One possible explanation is that of vector consumption, and another is the role of differential behavior, any vector behavior modified or adjusted by the infection, on the spread of infection. Specifically, we consider the increased frequency of feeding times of vectors whose salivary glands may be swollen and affecting the vectors' ability to swallow. Also, in the southeastern United States, *T. Sanguisuga*, *T. Cruzi's* primary vector in this region, has been observed wandering around in broad daylight, which is in contrast to the cool, dark hiding places where it usually resides. This behavior increases its vulnerability to predation by a host, and may be a result of any number of things, including perhaps neural dysfunction, or desperation in its search for food due to difficulty in feeding as a result of the first type of differential behavior discussed.

We use a deterministic mathematical model to examine the relationships in this system between vectors and hosts, revealing a system rich in dynamics. Sensitivity analysis is performed on this complex system to identify key factors in the maintenance of *T. Cruzi* in the sylvatic cycle. The significance of both types of differential behavior are examined

and compared. And finally, the role of vector consumption and its impact on the epidemic is discussed.

2 The Model

We focus on the infection of a single host species by a single vector species and vice versa. Since the size of the host population is effectively larger than that of the vectors, and the time scale does not permit significant variation in births and deaths, we assume the host population to be constant, or equivalently, that the birth and death rates are equal. This allows a reduction in model equations and the explicit examination of only the infected hosts, I_h, where the susceptible hosts can be readily obtained by the relationship $S_h(t) = N_h - I_h(t)$. Mortality due to infection is not included in our model as it has not been observed in either the mammalian hosts or the vectors. Once infection is acquired by either host or vector, it persists throughout its lifetime and therefore, no recovery has been included in our model.

Hosts can be infected by two modes of transmission - consumption of infected vectors and the traditional mode which is through the feces of the vector. Infections due to defecation following a bloodmeal are enhanced by any increased frequency in feeding of the infected vector upon the host, accounted for by the factor γ_1. Also, the probability of being bitten by an infected host is given by $\frac{\gamma_1 I_v}{S_v+\gamma_1 I_v}$. Consumption of vectors is taken as a monotone increasing and saturating density-dependent relationship, represented by $E_h(N_v) = \frac{BN_v}{A+N_v}$ with $N_v = S_v + I_v$. Infected vectors, which may tend to unwittingly wander into unprotected areas, are consumed at a greater rate than uninfected vectors. Therefore, the consumption rate is evaluated at $S_v + \gamma_2 I_v$ and the probability of encountering an infected vector is then $\frac{\gamma_2 I_v}{S_v+\gamma_2 I_v}$. Setting either γ_1 or γ_2 equal to 1 would be the exclusion of either type of differential behavior of vectors due to infection of *T.Cruzi*. Therefore, in all further analysis it is assumed that $\gamma_1, \gamma_2 \geq 1$. The model is given by:

$$\dot{I}_h(t) = \beta \frac{\gamma_1 I_v S_h}{S_v + \gamma_1 I_v} + \rho E_h[S_v + \gamma_2 I_v] \frac{\gamma_2 I_v S_h}{S_v + \gamma_2 I_v} - \mu_h I_h \tag{1}$$

$$\dot{S}_v(t) = r_v N_v (1 - \frac{N_v}{K}) - \mu_v S_v - \tilde{\beta} S_v \frac{I_h}{N_h} - E_h[S_v + \gamma_2 I_v] \frac{S_v N_h}{S_v + \gamma_2 I_v} \tag{2}$$

$$\dot{I}_v(t) = \tilde{\beta} S_v \frac{I_h}{N_h} - \mu_v I_v - E_h[S_v + \gamma_2 I_v] N_h \frac{\gamma_2 I_v}{S_v + \gamma_2 I_v} \tag{3}$$

Susceptible vectors are lost to natural death, death due to consumption, and infection due to biting an infected host. Vector growth is assumed to have a logistic form with r_v representing the intrinsic growth rate, K the carrying capacity, and μ_v the natural death rate. Infected vectors are assumed to die from only natural death and consumption by hosts. All other parameters are defined in table 1.

Parameter	Interpretation
β	per capita traditional transmission from vectors to hosts
$\tilde{\beta}$	per capita traditional transmission from hosts to vectors
ρ	per capita transmission rate of hosts due to consumption of infected vectors
γ_1	increased feeding frequency of vectors due to infection
γ_2	vectors' increased vulnerability to consumption by hosts as a result of infection
μ_h	natural death of hosts
μ_v	natural death of vectors
r_v	growth rate of vectors
K	carrying capacity of vector population
A	vector density at half-maximal consumption
B	maximal vector consumption rate

Table 1: Model Parameters

3 Analysis

3.1 Existence of Disease-Free Equilibria

It is important to first consider the dynamics of the hosts and vectors in the absence of infection before the introduction of an infection is logical. To find a disease-free equilibrium, we set the system of differential equations as well as the infective classes equal to zero. To begin, we consider the dynamics of the vectors without consumption by hosts.

$$\dot{S}_v(t) = r_v S_v(1 - \frac{S_v}{K}) - \mu_v S_v = 0 \tag{4}$$

Solving equation (4) for S_v gives $\bar{S}_v = (1 - \frac{\mu_v}{r_v})K$. We require that $r_v > \mu_v$ for $\bar{S}_v > 0$. Since with the inclusion of vector consumption by hosts, the nontrivial equilibria $S_v^* \leq \bar{S}_v$, we require this condition for the rest of the model analysis. For the full vector dynamics we begin by finding the equilibria of the following equation:

$$\dot{S}_v(t) = r_v S_v(1 - \frac{S_v}{K}) - \mu_v S_v - E_h[S_v]N_h$$

These roots are $S_{v0}^* = 0$ and
$S_{v1,2}^* = \frac{1}{2}\{K(1 - \frac{\mu_v}{r_v}) - A \pm \sqrt{(K(1 - \frac{\mu_v}{r_v}) - A)^2 - 4\frac{K}{r_v}(BN_h + (\mu_v - r_v)A)}$ with $S_{v1}^* \leq S_{v2}^*$. For these equilibria to be positive, and hence of biological relevance, $A < K(1 - \frac{\mu_v}{r_v})$, otherwise, the vectors go extinct since only the zero equilibrium exists in that case. If, however, $A < K(1 - \frac{\mu_v}{r_v})$, $\frac{BN_h}{(r_v - \mu_v)A} > 1$ and $(K(1 - \frac{\mu_v}{r_v}) - A)^2 > 4\frac{K}{r_v}(BN_h + (\mu_v - r_v)A)$, then both equilibria exist and are positive. It is also possible for the positive equilibria to coalesce, and this occurs when $(K(1 - \frac{\mu_v}{r_v}) - A)^2 = 4\frac{K}{r_v}(BN_h + (\mu_v - r_v)A)$, and then the vector-host system, in the absence of infection would have only 2 possible equilibria, S_{v0}^* and $S_{v1}^* = S_{v2}^*$.

3.2 Stability of Disease-Free Equilibria

The stability of the vector population in the absence of infection can be discussed via the examination of the following set of equations:

$$\begin{aligned} f(S_v) &= \dot{S}_v(t) = r_v S_v(1 - \frac{S_v}{K}) - \mu_v S_v - E_h[S_v]N_h \\ f'(S_v) &= r_v(1 - \frac{S_v}{K}) - \frac{r_v S_v}{K} - \mu_v - \frac{BN_h(A + S_v) + BS_v N_h}{(A + S_v)^2} \\ f''(S_v) &= \frac{-2r_v}{K} - BN_h(\ln|A + S_v| + \frac{A^2 + AS_v - S_v^2}{(A + S_v)^4}) \end{aligned}$$

To examine the local stability of $S^*_{v_0} = 0$ we consider the sign of $f'(0) = r_v - \mu_v - \frac{BN_h}{A}$. This expression is positive for $\frac{r_v}{\mu_v + \frac{BN_h}{A}} > 1$, and thus extinction of the vector population is unstable. Similarly, $f'(0) < 0$ for $\frac{r_v}{\mu_v + \frac{BN_h}{A}} < 1$, and then $S^*_{v_0} = 0$ is then locally asymptotically stable. This quantity can be interpreted as the ratio of vector births to death due to natural causes and consumption. So it agrees with our intuition that if the dynamics of the population are such that this ratio is larger than 1, the vectors will not become extinct, and if this ratio is less than 1, the vectors will become extinct. Therefore, we assert that $\mathcal{R}_d = \frac{r_v}{\mu_v + \frac{BN_h}{A}}$ is the demographic reproduction number of the vector population.

$f(S_v)$ and $f'(S_v)$ are both continuous and smooth functions. Therefore, when $\mathcal{R}_d > 1$ we have that $f'(0) > 0$ and when $f(S_v)$ reaches the next zero, $S^*_{v_2}$, ($S^*_{v_1} < 0$ here) it is decreasing, or equivalently, $f'(S^*_{v_2}) < 0$. This implies that $S^*_{v_2}$ is locally asymptotically stable. Similarly, if $\mathcal{R}_d < 1$, $f'(0) < 0$, so extinction becomes a stable equilibrium and the function $f(S_v)$ is increasing when it reaches $S^*_{v_1}$, and hence $f'(S^*_{v_1}) > 0$ and this first equilibrium is unstable. In this case, $S^*_{v_2}$ is locally asymptotically stable due to $f'(S^*_{v_2}) < 0$.

The demographic reproductive number is a threshold parameter, which can be interpreted as describing the likelihood of the extinction of the population. Typically, $\mathcal{R}_d < 1$ represents the case where $S^*_{v_0} = 0$ is stable and therefore extinction is likely. When $\mathcal{R}_d$ increases and becomes greater than 1 $S^*_{v_0} = 0$ undergoes transcritical bifurcation and becomes unstable, and a positive equilibrium becomes stable. However, for this model, there exists a range of parameters where $\mathcal{R}_d < 1$ and the population reaches a stable positive equilibrium. Figure 1, which displays this backward bifurcation, plots the equilibria for the specified set of parameters versus their corresponding $\mathcal{R}_d$ values as the vector growth rate varies between 0.5 and 2 births per year.

As shown in Figure 1 it is possible to have $\mathcal{R}_d < 1$, but if $(K(1 - \frac{\mu_v}{r_v}) - A)^2 > 4\frac{K}{r_v}(BN_h + (\mu_v - r_v)A)$ and $S_v(0) > S^*_{v_1}$, the population will go to $S^*_{v_2}$ instead of dying out as would be predicted from the reproduction number alone. Specifically, when $\mathcal{R}^*_d = 1 - \frac{K}{r_v}\frac{((K(1-\frac{\mu_v}{r_v})-A)^2}{BN_h + \mu_v A}$, the positive equilibria coalesce, and we observe that if $\mathcal{R}_d > \mathcal{R}^*_d$ and

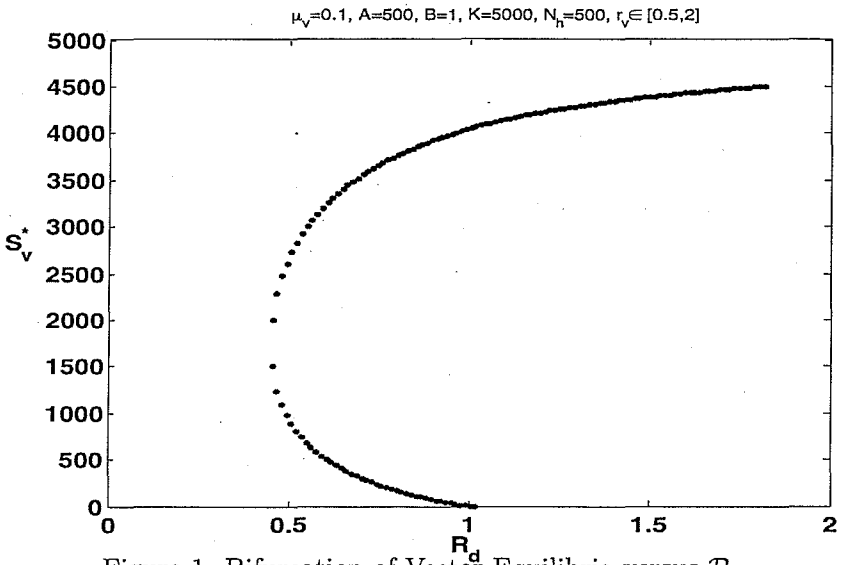

Figure 1: Bifurcation of Vector Equilibria versus $\mathcal{R}_d$

$S_v(0) > S^*_{v_1}$ the vector population will go to $S^*_{v_2}$. If, however, $\mathcal{R}_d < 1$ and $(K(1 - \frac{\mu_v}{r_v}) - A)^2 > 4\frac{K}{r_v}(BN_h + (\mu_v - r_v)A)$ but now $S_v(0) < S^*_{v_1}$ the vectors will become extinct as predicted. Thus, in this system, $\mathcal{R}_d$ fails as the sole threshold parameter, predicting the outcome of the steady state vector size, and it is necessary to consider the initial conditions as well.

Figure 2 shows the disease-free vector population dynamics, including consumption by a constant host population, for varied rates of growth. These different rates of growth were chosen to demonstrate the behavior illustrated in Figure 1. For $r_v = 0.5$, $\mathcal{R}_d < 1$ and the vector population quickly dies out as expected. However, when r_v is increased to 0.8, $\mathcal{R}_d$ remains less than one, but the vector population reaches a positive steady state. In this case, the initial condition of the system is such that it falls between the two equilibria, $S^*_{v_1}$ and $S^*_{v_2}$. When r_v is sufficiently increased to achieve a $\mathcal{R}_d > 1$, this parameter again becomes an indicator of the vector population level, which reaches a positive steady state as expected.

Figure 3 further demonstrates the situation where although the threshold parameter indicates vector extinction as a stable steady state, a positive vector population is the long-term result. This is a result of both roots being positive in this parameter regime and also the initial condition $S_v(0) > S^*_{v_0}$.

3.3 Basic Reproductive Number, $\mathcal{R}_0$

The basic reproductive number of the infection, $\mathcal{R}_0$, interpreted as the average number of secondary infections, is a threshold parameter, indicative of the onset of an epidemic as a result of the introduction of an infection to a disease-free population. From the

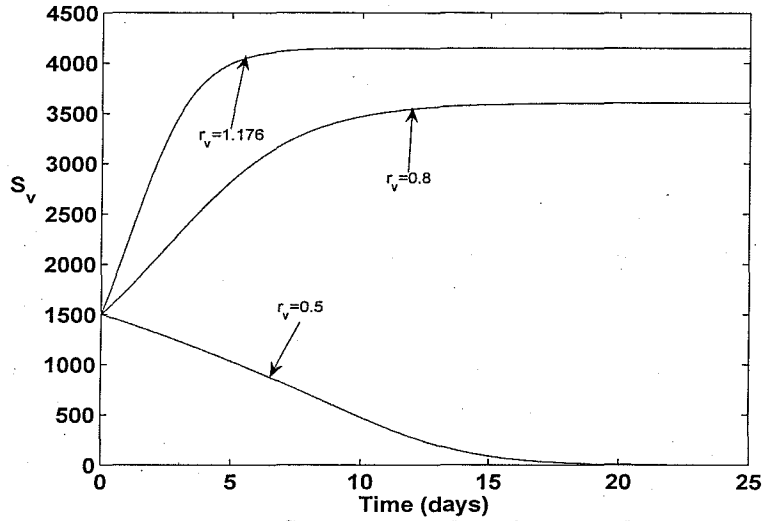

Figure 2: System Equilibria for Varied r_v

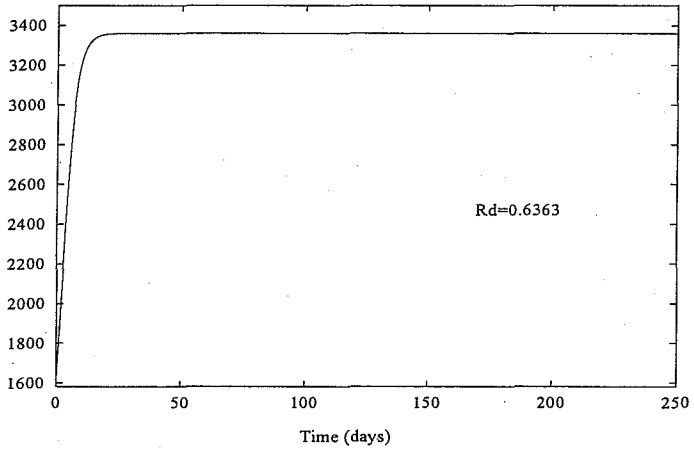

Figure 3: Positive Equilibrium with $\mathcal{R}_d < 1$

disease-free analysis it is evident that it is possible to have two positive stable vector population sizes, although not simultaneously. Therefore, by the method discussed in [4], we calculate this parameter as a function of the relevant stable vector size depending on the initial conditions and parameter values.

$$\mathcal{R}_0 = \sqrt{\frac{\tilde{\beta}}{\mu_h}\frac{\beta\gamma_1 + \rho\gamma_2 E_h[S_v^*]}{\mu_v + \gamma_2 \frac{N_h}{S_v^*} E_h[S_v^*]}} = \sqrt{\mathcal{R}_1 \mathcal{R}_2}$$

$\mathcal{R}_1$ is the number of vector infections produced per infective host for the time they are infective, which is $\frac{1}{\mu_h}$ since hosts die only due to natural causes. $\mathcal{R}_2$ represents the secondary host infections produced per infective vector introduced for the duration of the time that they are infective. This period is represented by $\frac{1}{\mu_v + \gamma_2 \frac{N_h}{S_v^*} E_h[S_v^*]}$ since vectors can die due to natural causes or through consumption by hosts.

It is worthwhile to compare the reproductive numbers and hence, compare the severity of a possible epidemic, corresponding to each stable disease-free vector size. Since $\frac{B}{A+S_{v_1}^*} \geq \frac{B}{A+S_{v_2}^*}$, $\frac{1}{\mu_v + \gamma_2 N_h \frac{B}{A+S_{v_1}^*}} \leq \frac{1}{\mu_v + \gamma_2 N_h \frac{B}{A+S_{v_2}^*}}$. Also, since $E_h[S_v]$ is a monotone increasing function, $\rho\gamma_2 E_h[S_{v_1}^*] \leq \rho\gamma_2 E_h[S_{v_2}^*]$, and we have that

$$\mathcal{R}_0(S_{v_1}^*) = \sqrt{\frac{\tilde{\beta}}{\mu_h}\frac{\beta\gamma_1 + \rho\gamma_2 E_h[S_{v_1}^*]}{\mu_v + \gamma_2 \frac{N_h}{S_{v_1}^*} E_h[S_{v_1}^*]}} \leq \sqrt{\frac{\tilde{\beta}}{\mu_h}\frac{\beta\gamma_1 + \rho\gamma_2 E_h[S_{v_2}^*]}{\mu_v + \gamma_2 \frac{N_h}{S_{v_2}^*} E_h[S_{v_2}^*]}} = \mathcal{R}_0(S_{v_2}^*).$$

For any given set of parameters, an epidemic grows much more quickly if the vector population size is larger. However, since the two population sizes are not stable simultaneously, or bistable, further investigation into this question is warranted. While in most cases it is clear how the parameters will affect $\mathcal{R}_0$, it is not clear which of these have the strongest effect, either positive or negative.

3.4 Sensitivity of $\mathcal{R}_0$ to parameters

In an effort to quantify the effect of changes in parameters on the value of $\mathcal{R}_0$, we compute the sensitivity indices of $\mathcal{R}_0$ with respect to certain key parameters from the model. For the sensitivity of a solution u to a parameter, p, its sensitivity index is defined as

$$S_p = \frac{\frac{\partial u}{u}}{\frac{\partial p}{p}} = \frac{p}{u}\frac{\partial u}{\partial p}$$

provided $u \neq 0$. This definition was used to compute all of the indices displayed in Table 2. While the indices displayed in the table are as simplified as much as possible, they still do not lend themselves readily to quantitative analysis. Therefore, numerical estimates for model parameters, Table 3, were used to determine which parameters had stronger effects on $\mathcal{R}_0$, and thus the spread of the epidemic.

The parameter A is shown to have the largest (in magnitude) positive sensitivity index of $\mathcal{R}_0$, indicating that $\mathcal{R}_0$ increases the most by the least change in A relative to the other parameters. This, taken together with the fact that the most negative sensitivity index of

p	S_p
γ_1	$\frac{\mathcal{R}_0}{2\sqrt{\mu_h}+2\frac{\rho\gamma_2}{\gamma_1\beta}E_h[S_v^*]}$
γ_2	$\frac{1}{2}\gamma_2 E_h[S_v^*]\left(\frac{\rho}{\frac{\beta\gamma_1}{E_h[S_v^*]}+\rho\gamma_2}-\frac{\frac{N_h}{S_v^*}}{\frac{\mu_v}{E_h[S_v^*]}+\frac{\gamma_2 N_h}{S_v^*}}\right)$
β	$\frac{B}{2\mathcal{R}_0^2}\frac{\beta}{\mu_h}\frac{\gamma_1}{\mu_v+\gamma_2\frac{N_h}{S_v^*}E_h[S_v^*]}$
$\tilde{\beta}$	$\frac{1}{2}$
ρ	$\frac{\rho}{2\mathcal{R}_0^2}\frac{\tilde{\beta}}{\mu_h}\left(\frac{\gamma_2 E_h[S_v^*]}{\mu_v+\gamma_2\frac{N_h}{S_v^*}E_h[S_v^*]}\right)$
r_v	$\frac{r_v}{2\mathcal{R}_0^2}\frac{\partial S_v^*}{\partial r_v}[Z]$
μ_v	$\frac{\mu_v}{2\mathcal{R}_0^2}\frac{\partial S_v^*}{\partial \mu_v}\left[\frac{\frac{\tilde{\beta}}{\mu_h}\rho\gamma_2 E_h'[S_v^*]-\mathcal{R}_0^2(1+\gamma_2 N_h B ln\lvert A+S_v^*\rvert)}{\mu_v+\gamma_2\frac{N_h}{S_v^*}E_h[S_v^*]}\right]$
μ_h	$\frac{1}{2}\mu_h^2 ln\lvert\mu_h\rvert$
A	$\frac{A}{2\mathcal{R}_0^2}\frac{\partial S_v^*}{\partial A}[Z]$
B	$\frac{B}{2\mathcal{R}_0^2}\frac{\partial S_v^*}{\partial B}[Z]$

Table 2: Sensitivity Indices S_p of $\mathcal{R}_0$ to model parameters, p, where $Z = \frac{\frac{\tilde{\beta}}{\mu_h}\rho\gamma_2 E_h'[S_v^*]-\mathcal{R}_0^2\gamma_2 N_h B ln\lvert A+S_v^*\rvert}{\mu_v+\gamma_2\frac{N_h}{S_v^*}E_h[S_v^*]}$

Parameter	Estimate	Range	Sensitivity of $\mathcal{R}_0$	Range
β	0.2	0.05-0.3	157	3.65 - 268.05
$\tilde{\beta}$	0.5	0.3-0.7	$\frac{1}{2}$	$\frac{1}{2}$
ρ	0.002	0.000001 - 1	0.008	0.00000403 - 0.4447
γ_1	1	1-5	322	322-715
γ_2	1	1-5	-0.9613	-0.9- (-3.3)
μ_h	0.000685	0.000548-0.000913	-1.70×10^{-6}	$-1.13\times10^{-6}--2.92\times10^{-6}$
μ_v	0.00588	0.00526-0.0066	322	322 - 715
r_v	1.176	0.5-2	0.00958	0.005-0.332
A	1000	500-2000	2.47×10^{10}	0.6-9
B	2	1-15	-5510	-1583 - - 10380

Table 3: Model Parameters

$\mathcal{R}_0$ is with respect to B, indicates that consumption dynamics play the most important role in the spread of an epidemic. Specifically, A, which is the vector population size at which the consumption rate is half-maximal, affects the threshold parameter in a positive way. A small increase in B, the maximal consumption rate of vectors by hosts, is then predicted to have the effect of greatly decreasing the threshold parameter. In other words, if hosts eat fewer vectors at smaller population levels, onset of an epidemic is less likely,

and this mode of transmission is being slowed. Seemingly in contrast, the sensitivity index of B indicates that less vector consumption has a positive effect on the spread of an epidemic. However, too great of an increase in B is shown to deplete the vector population in simulation, and therefore not a realistic scenario.

When comparing the sensitivity indices of γ_1 with γ_2, we notice γ_1 seems to have a positive effect on $\mathcal{R}_0$, indicating that an increase in this parameter, or increased frequency of bloodmeals due to infection of vectors, enhances the onset and/or likelihood of an epidemic. In contrast, the sensitivity index of $\mathcal{R}_0$ with respect to γ_2 indicates that an increase in vectors' vulnerability to predation hinders the spread of infection, due to the infected vectors being depleted from the vector population at a preferential rate as compared to the susceptibles.

4 Numerical Results

While the reproductive number usually provides a good indicator of the onset of an epidemic, the full numerical solution to a system provides a more direct approach for examining differential behavior and consumption dynamics.

With the parameters set as given in Table 3, a typical solution of the system is shown below. The system reaches endemic equilibrium at about 40 days, with the susceptible vector population at significantly lower levels than the infective vector population. In the endemic state, the infective hosts approach the total number of hosts, indicating that almost all the hosts are infective. The disparity in these prevalence levels with those observed can be explained by the lack of reliability and in many cases of measurability in parameter values. However, the current model and parameters provide us with a reliable platform to study the dynamics of the system as well as the effects of consumption dynamics and differential behavior.

4.1 Sensitivity of Solutions to Parameters

Using Berkeley Madonna, we were able to numerically calculate $\frac{\partial u}{\partial p}$ as a function of time for all of the parameters. This partial derivative was multiplied by the parameter and divided by the numerical solution at the same time step. In this way, a time course of the sensitivity index was calculated and is displayed for several parameters of interest below. All parameters are the same as those shown in 4 unless otherwise stated.

In Figures 5 through 7, relative changes in the solution are displayed as a result of small changes in the initial conditions. Notice that shortly after 50 days, changes in the initial conditions have no effect on the solution, and in other words, the equilibrium reached by the system does not change drastically if we use slightly different initial conditions. This effect we would expect from the notion of a stable steady state. We notice that an increase in $I_h(0)$ seems to have the strongest effect on all three variables and for a longer period of time. These figures show that an increase would serve to initially increase the number of

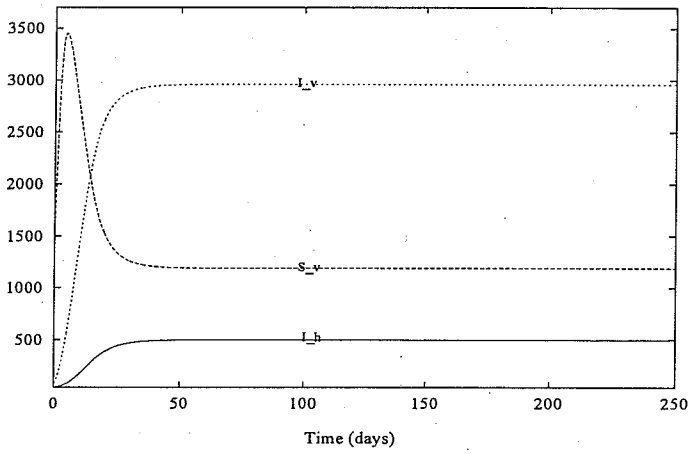

Figure 4: Simulation with Estimated Parameters: $\beta = 0.2, \tilde{\beta} = 0.5, \rho = 0.002, N_h = 500, K = 5000, \mu_h = 0.00685, A = 1000, B = 2, \mu_v = 0.00588, r_v = 1.176, \gamma_1 = \gamma_2 = 1$, $\mathcal{R}_d = 1.169$

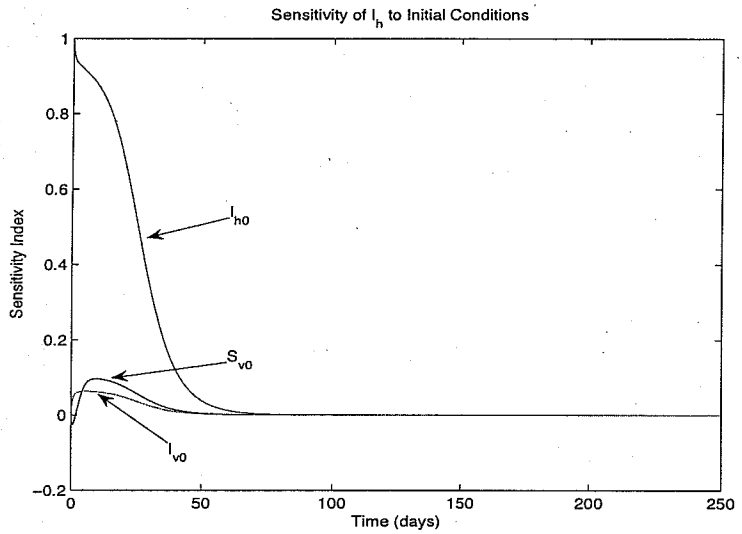

Figure 5: Sensitivity of I_h to Initial Conditions

infective vectors, which would reinforce an increase in the number of infective hosts, and of course this would then deplete the number of susceptible vectors.

The effects of differential behavior on the full solution of the system are quantified and compared in Figure 8 and Figure 9. These results agree with our sensitivity analysis of

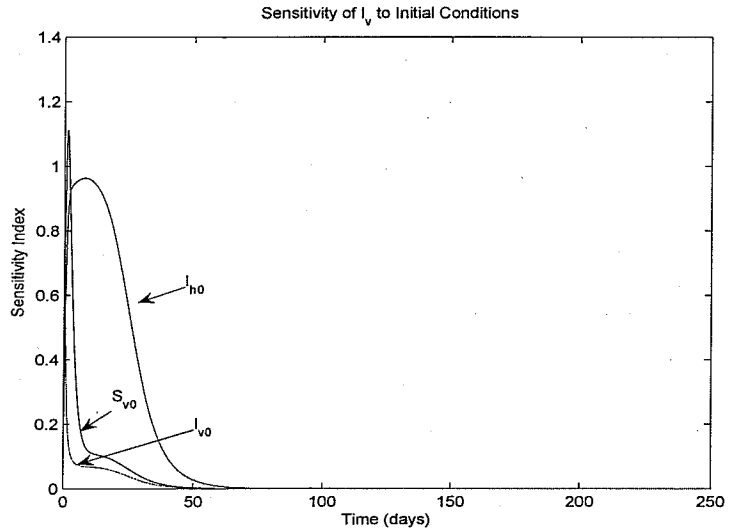

Figure 6: Sensitivity of I_v to Initial Conditions

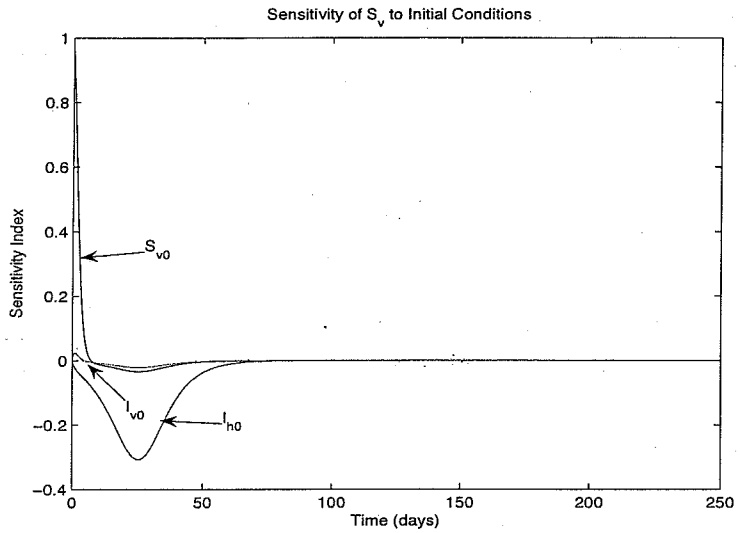

Figure 7: Sensitivity of S_v to Initial Conditions

$\mathcal{R}_0$ previously, in that small positive changes in γ_1 produce positive changes in the time courses of both infective hosts and vectors, while small positive changes in γ_2 produce negative changes in the time courses of infective populations. The quantitatively opposite effect was observed in the susceptible vector population, and hence was omitted as no additional insight was gained.

Figures 10 and 11 display the sensitivities of the infectives' solutions to small changes

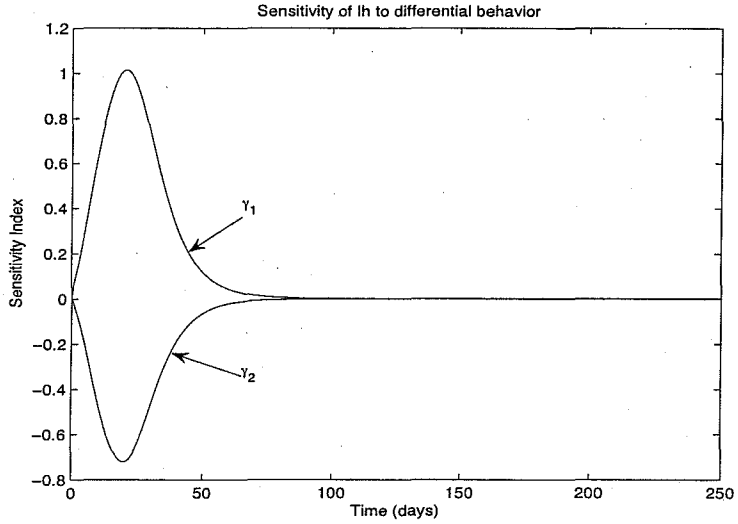

Figure 8: Sensitivity of I_h to Differential Behavior

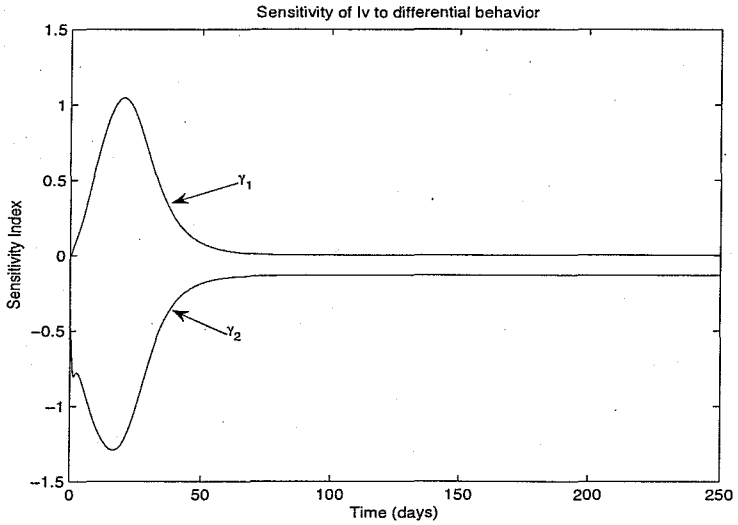

Figure 9: Sensitivity of I_v to Differential Behavior

in parameters governing vector population dynamics. These include the growth and death rates of the vectors and hosts as well as the constants determining the consumption rates of the vectors. Changes in the mortality rates of both vectors and hosts seem to not affect the gain or loss of infective vectors and hosts significantly. In direct contrast, increasing B slightly, the maximal consumption rate, would greatly decrease the infective hosts, although not affect the population level present at equilibrium. Not surprisingly,

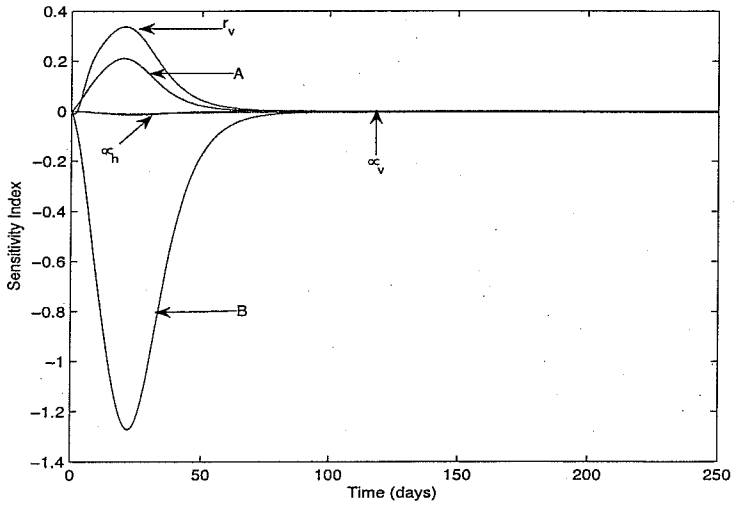

Figure 10: Sensitivity of I_h to Parameters Governing Population Dynamics

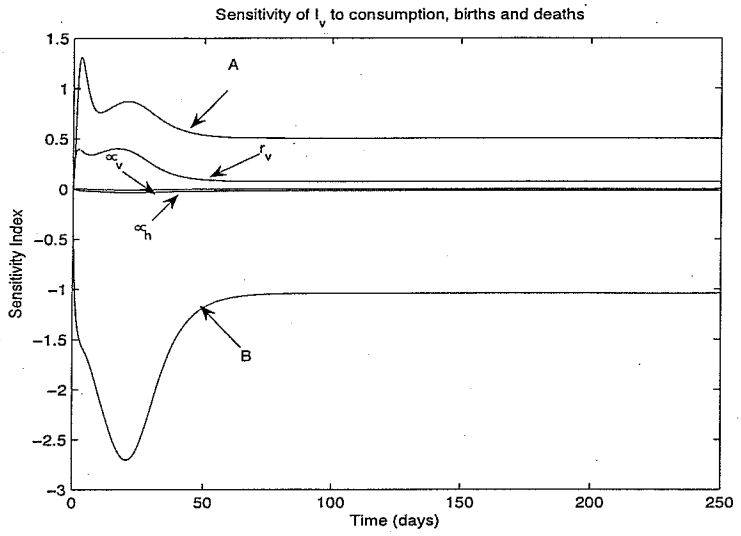

Figure 11: Sensitivity of I_v to Parameters Governing Population Dynamics

the infective vectors are also most affected by small increases in B, and in a negative way. However, the vectors' steady state population is also decreased by these changes. Increasing slightly the growth rate of the vectors, r_v, and the population level at which the consumption rate is half-maximal A, results in increasing infective vectors and hosts. The stable population level of the hosts again is unaffected, while the steady state vector level is decreased. Increasing the growth rate would serve to increase the pool of vectors

that could get infected and then infect hosts. Given that the prevalence level in the host population is near saturation, the elevated infection in the host populations will not be observed. Increasing A effectively slows down the consumption rate, increasing the vector population size at which greater consumption rates occur. This effect is similar to that of an increased growth rate since both serve to increase the pool of vectors.

4.2 Effect of Vector Consumption

After having determined which parameters will affect the solutions of the system most significantly with small relative changes, we explore the parameter space for greater changes in these parameters.

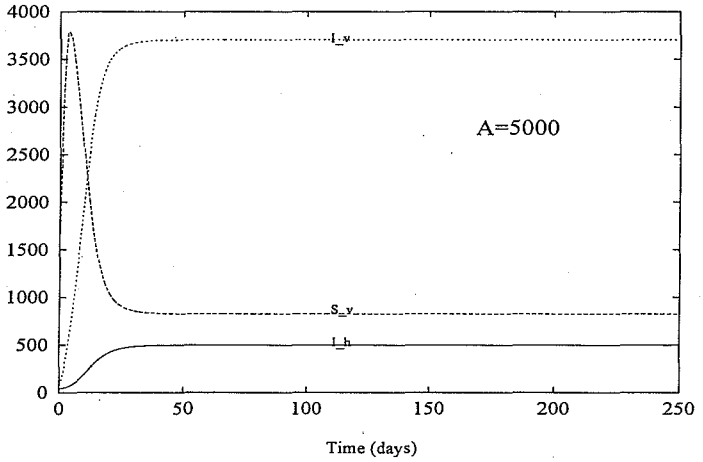

Figure 12: A=5000, B=5, $\gamma_1 = \gamma_2 = 1$, $\mathcal{R}_d = 5.71$

As A increases, the vector population required for greater consumption rates, increases. This increases the pool of vectors to carry infection initially, since they are consumed at a lower rate. However, as the vector size increases, the consumption rate increases until a steady state is reached. This greater total vector population at endemic steady state is reached more quickly than that at lower levels of A. The rate at which the system reaches endemic equilibrium is a result of the rate of initial spread of infection, related to the magnitude of $\mathcal{R}_0$, which we have seen increases with increasing values of this parameter. The prevalence levels, however, are unchanged, as the increased infective vector levels are accompanied by a similar increase in susceptible vectors.

Increasing the maximal consumption rate slightly results in significantly less infective vectors, and more susceptible vectors at steady state, resulting in lower prevalence levels, and a slightly lower total vector population. If B is increased slightly more, by only one vector per day, initially the infection is suppressed , but consumption becomes a

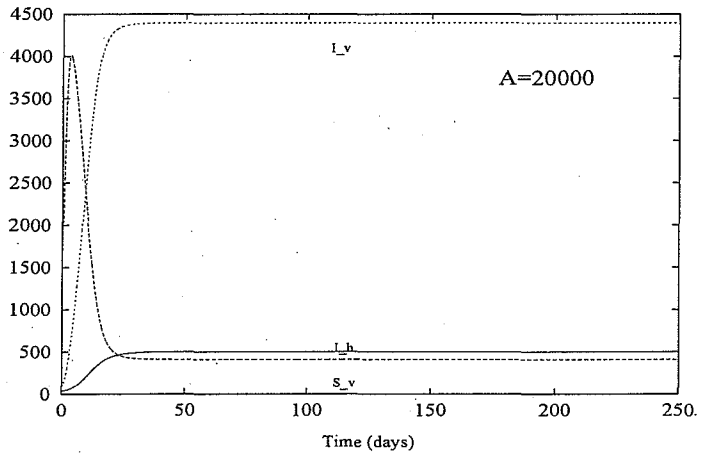

Figure 13: A=20000, B=5, $\gamma_1 = \gamma_2 = 1$, $\mathcal{R}_d = 8.98$

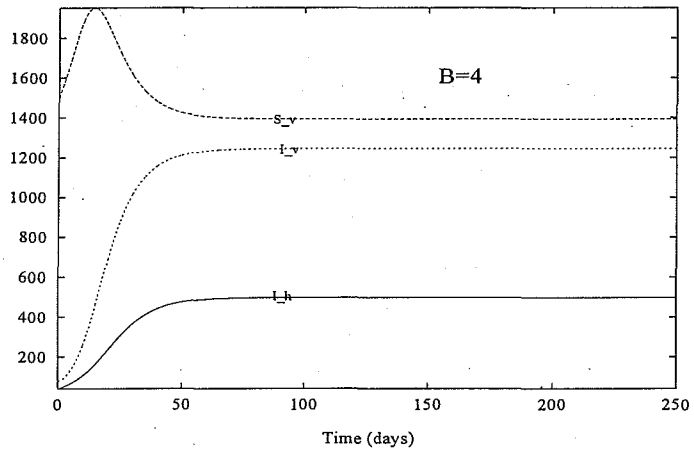

Figure 14: B=4, A=1000, $\gamma_1 = \gamma_2 = 1$, $\mathcal{R}_d = 0.586$

dominating factor in vector population dynamics, pushing $\mathcal{R}_d$ below the threshold for a stable positive equilibrium according to Figure 1. While it seems unnatural to consult a diagram of disease-free equilibria for a system in the presence of infection, it is possible if the plotted equilibria are taken as representing the total vector population when the system is in the endemic state.

In fact, upon inspection of Figures 16 and 17, we see that if the susceptible and

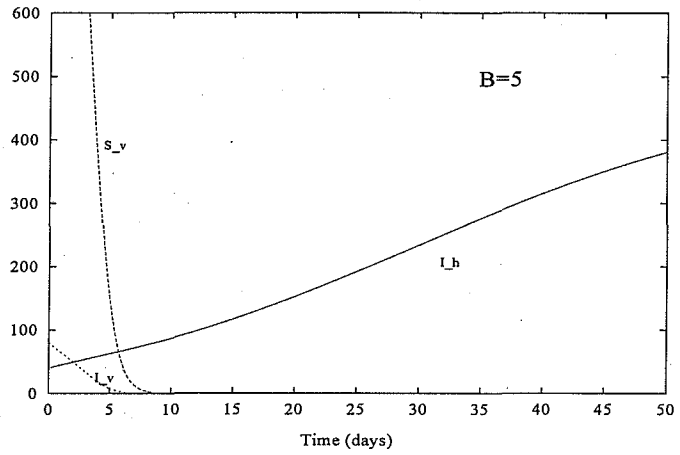

Figure 15: B=5, A=1000, $\gamma_1 = \gamma_2 = 1$, $\mathcal{R}_d = 0.469$

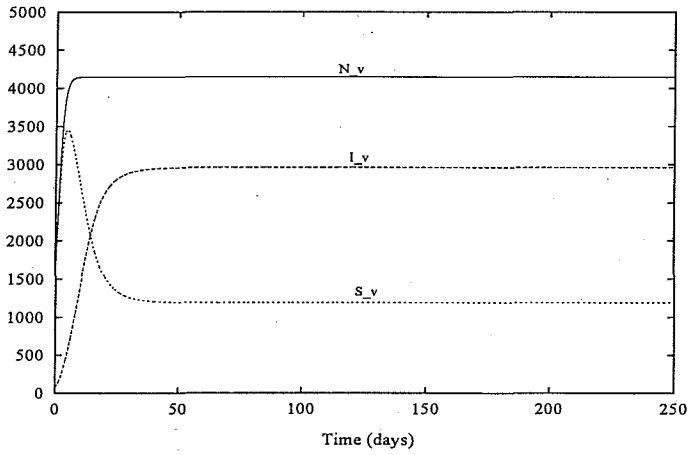

Figure 16: A typical time course of the total vector population to reach endemic equilibrium.

infective vectors are summed during the course of a typical infection (Figure 16), the result is identical to that of the susceptible vector population in the disease-free case (Figure 17). This is due to the lack of deaths as a result of infection (according to model assumptions). Thus, in the discussion of the effects of the population dynamics on this system it is worthwhile to consider the demographic reproductive number, $\mathcal{R}_d$.

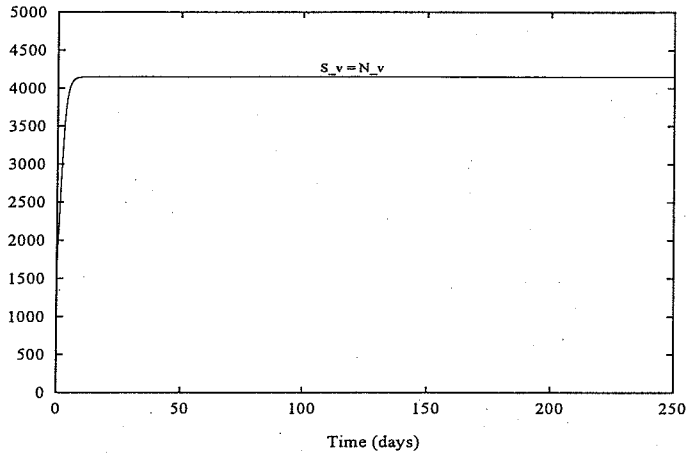

Figure 17: A typical time course of the vector population to reach the disease-free equilibrium.

4.3 Differential Behavior Effects

We have shown with sensitivity analysis of $\mathcal{R}_0$ and the solution of the full system that the outcome of the disease is sensitive to changes in small changes in γ_1 and γ_2, the measures of differential behavior. The question of how the system behaves if the vectors are affected substantially by the parasite is addressed in this section.

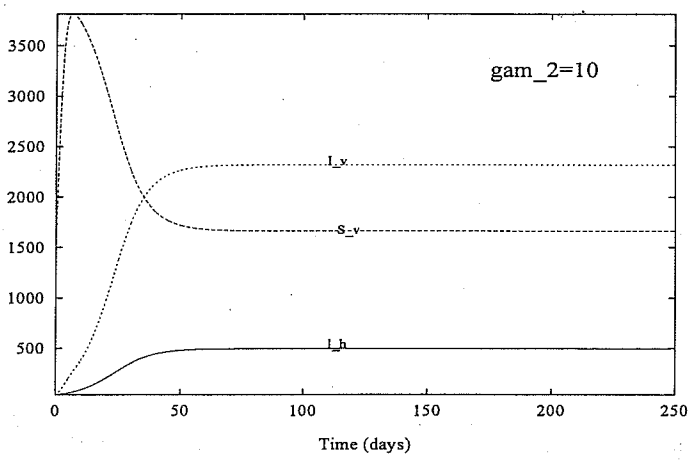

Figure 18: $\gamma_2 = 10, B = 2, \gamma_1 = 1$

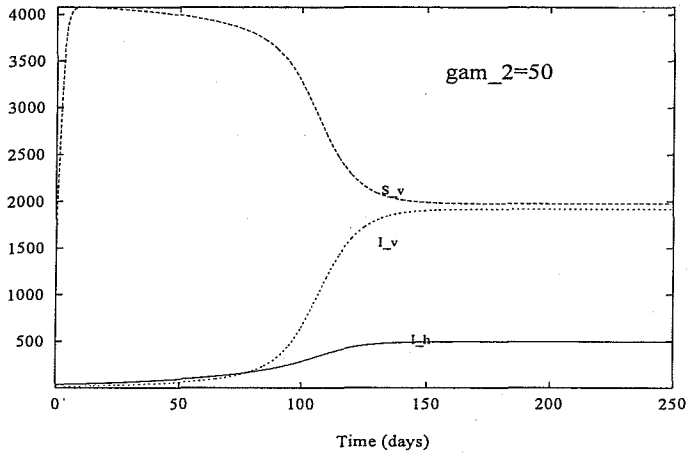

Figure 19: $\gamma_2 = 50, B = 2, \gamma_1 = 1$

Increasing γ_2, or simulating the situation of the vectors being exposed to predation as a result of infection, results in lower levels of infective vectors and a corresponding increase in susceptible vectors at the endemic state. Any increase in $\gamma_2 > 1$ effectively increases the consumption rate of vectors affecting the population dynamics of the vectors and reducing their steady state level. However, infectives are preferentially consumed, indicating that it is no longer useful to discuss the disease-free situation as a predictor for the total vector population. However, it is clear that increasing γ_2 and B, the maximal vector consumption rate, similarly affect the population and disease dynamics. However, since the susceptibles are not consumed at a greater rate, the system is not as sensitive to changes in this parameter. Also, even for unrealistically high values of this parameter, the system is not driven to extinction.

γ_1 measures the increased feeding frequency in response to the vectors' difficulty in swallowing when infected with *T. Cruzi*, increasing the contact rate between the hosts and vectors that results in infection of hosts. In Figures 20 and 21, we see that increasing this parameter increases the infected vectors and decreases the susceptible vectors at the endemic level. The rate at which endemic equilibrium is reached is accelerated, as is expected since small changes in this parameter had the effect of increasing $\mathcal{R}_0$.

5 Conclusions and Discussion

In this discussion of the sylvatic cycle of *T. Cruzi*, we have explored the roles of vector consumption and two types of differential behavior and their implications for disease dynamics. Previous modeling efforts on Chagas' disease have focused on the host-vector system involving humans as hosts. This system does not take into account the high prevalence

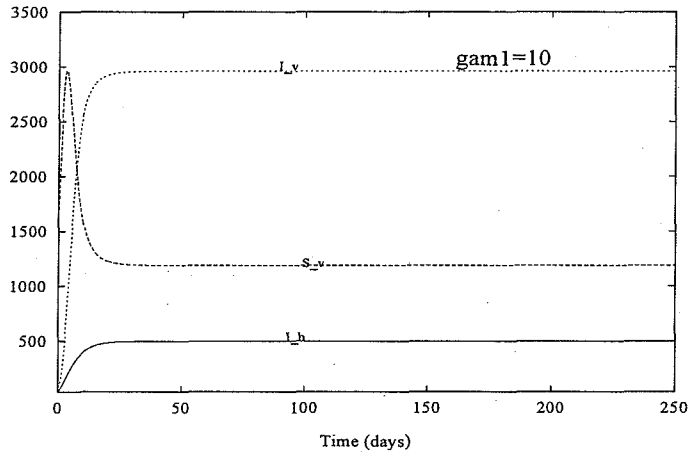

Figure 20: $\gamma_1 = 10, B = 2, \gamma_2 = 1$

levels observed in other mammals and clearly does not include any vector consumption, which we have shown very significantly affects the dynamics of disease spread.

A smooth saturating curve was used to estimate the rate of vector consumption as a function of vector population size. The two parameters, A and B, that determine the shape of this curve have been shown to be the most influential in determining both the initial spread of infection, and the endemic equilibrium. A represents the vector population size at which the vectors are consumed at half of the maximum rate. Increasing or decreasing this value has been shown to affect how quickly the system reaches the endemic state, although it does not affect the total vector population size. An increase in the maximal vector consumption rate, B, has been shown to decrease the number of vectors present at equilibrium, both disease-free and endemic. Through simulation, we have seen that increasing the rate at which vectors are consumed more strongly induces the extinction of vectors than boosting infection levels of hosts, likely due to the low probability of transmission. Since increasing B reduces the demographic reproductive number, if $\mathcal{R}_d < \mathcal{R}_d^*$ this could induce extinction of the vectors. This rate, however, is an intrinsic property of the animal consuming the vectors, and as such will not be affected by external means. Realistically, in any region, there are many mammals that consume this vector, and this result suggests that if a host with a high maximal consumption rate were present in the system at sufficiently high levels, the vector population could be driven to extinction.

Part of the motivation for this research was to determine how the differential behavior of the vectors induced by infection affected the spread of disease. Additionally, we would like to ascertain if this was enough to induce and maintain the otherwise unexplainable relatively high prevalence levels observed in the southeastern United States. Increasing

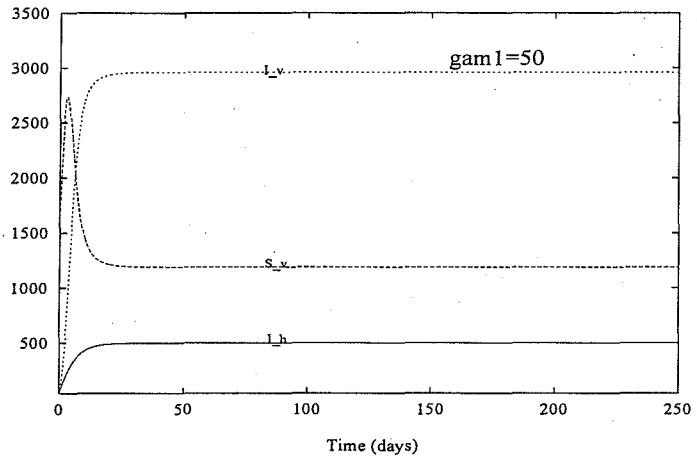

Figure 21: $\gamma_1 = 50, B = 2, \gamma_2 = 1$

the rate at which infective vectors are consumed, or in the context of the model, increasing γ_2 to be greater than one, serves not to increase the prevalence levels of infection, but to decrease the pool of infective vectors, thus hindering the spread of disease. This consumption increase is not strong enough to drive the vectors to extinction, but does serve to slightly decrease the population size at endemic equilibrium. Increased feeding frequency of vectors has been shown to not only significantly increase the threshold parameter for the existence of an epidemic, $\mathcal{R}_0$, but also increases the prevalence levels once an endemic state is reached. Therefore, we can conclude that increased feeding frequency is aiding in the maintenance of the high prevalence levels observed, while increased consumption of infective vectors is actually decreasing these levels.

References

[1] A. C. Aufderheide, W. Salo, M. Madden, J. Streitz, J. Buikstra, F. Guhl, B. Arriaza, C. Renier, L.E. Wittmers Jr, G. Fornaciari, M. Allison. A 9,000-year record of Chagas' disease, *Proc. Natl. Acad. Sci. USA* 101(7): 2034-9, 2004 Feb 17.

[2] C. Barnabé, R. Yaeger, O. Pung, M. Tibayrene. *Trypanosoma cruazi*: a considerable phylogenetic divergence indicates that the agent of Chagas disease is indigenous to the native fauna of the United States, *Exp. Parasitol.* 99(2): 73-79, 2001 Oct.

[3] S. F. Breniére, S. Pietrokovsky, E. Magallón Gastélum, M.-F. Bosseno, M. M. Soto, A. Ouaissi, F.L. Kasten, C. Wisinevsky-Colli. Feeding patterns of Triatoma longipennis

Usinger (Hemiptera, Reduviidae) in peridomestic habitats of a rural community in Jalisco State, Mexico, *J. Med. Entomol.* 41(6): 1015-1020, 2004 Nov.

[4] C. Castillo-Chávez, Z. Feng, W. Huang. On the Computation of $\mathcal{R}_0$ and its Role on Global Stability.

[5] Center for Disease Control, 2004. Chagas Disease Fact Sheet, http://www.cdc.gov/neidod/dpd/parasites/chagasdisease/factsht.chagas.disease.htm

[6] R.D. Holbert, E. Magiros, C.P. Hirsch, S.J. Nunenmacher. Chagas' disease: a case in south Mississippi, *J. Miss. State Med. Assoc.* 36(1): 1-5, 1995 Jan.

[7] D.A. Leiby, R.M. Herron Jr., E.J. Read, B. A. Lenes, R.J. Stumpf. *Trypanosoma cruzi* in Los Angeles and Miami blood donors: impact of evolving donor demographics on seroprevalence and implications for transfusion transmission, *Transfusion* 42(5): 549-555, 2002 May.

[8] S.M. Pietrzak, O.J. Pung. Trypanosomiasis in raccoons from Georgia, *J. Wildlife Disease* 34(1): 132-136, 1998 Jan.

[9] R. Vetter, Kissing bugs (Triatoma) and the skin. *Dermatology Online Journal* 7(1): 6, 2001.

[10] S. F. Wood, Importance of feeding and defecation times of insect vectors in transmission of Chagas diseases, *J. Economic Entomol.* 44: 52-54, 1951.

6 Appendix

Additional quantities used in the calculation of sensitivity of $\mathcal{R}_0$ to model parameters:

$$
\begin{aligned}
Disc &= (K(1-\frac{\mu_v}{r_v})-A)^2 - 4\frac{K}{r_v}(BN_h + (\mu_v - r_v)A) \\
\frac{\partial S_v^*}{\partial \mu_v} &= -\frac{1}{2}\frac{K}{r_v}(1 \pm \frac{1}{2}(Disc)^{-\frac{1}{2}}(2K(1-\frac{\mu_v}{r_v}) - 6A) \\
\frac{\partial S_v^*}{\partial r_v} &= -\frac{1}{2}\{lnr_v \pm \frac{1}{2}(Disc)^{-\frac{1}{2}}[(2A - 2K(1-\frac{\mu_v}{r_v})(K\mu_v lnr_v) - 4Klnr_v(BN_h + \mu_v A)]\} \\
\frac{\partial S_v^*}{B} &= \pm\frac{1}{2}(Disc)^{-\frac{1}{2}}(-4N_h\frac{K}{r_v}) \\
\frac{\partial S_v^*}{A} &= -\frac{1}{2}\{\frac{1}{A} \pm \frac{1}{2}(Disc)^{-\frac{1}{2}}(2A - 2K(1-\frac{\mu_v}{r_v})) + 4KA) \\
E_h'[S_v^*] &= \frac{AB}{(A+S_v^*)^2} \\
\frac{\partial}{\partial S_v^*}\Big[\frac{E_h[S_v^*]}{S_v^*}\Big] &= Bln|A+S_v^*|
\end{aligned}
$$